ASMS

RESEARCH ARTICLE

Graphene Oxide as a Novel Evenly Continuous Phase Matrix for TOF-SIMS

Lesi Cai,[1] Linfeng Sheng,[2] Mengchan Xia,[1] Zhanping Li,[1] Sichun Zhang,[1] Xinrong Zhang,[1] Hongyuan Chen[2]

[1]Department of Chemistry, Beijing Key Laboratory of Microanalytical Methods and Instrumentation, Tsinghua University, Beijing, 100084, People's Republic of China
[2]School of Chemistry and Chemical Engineering, State Key Laboratory of Analytical Chemistry for Life Science and Collaborative Innovation Center of Chemistry for Life Science, Nanjing University, Nanjing, 210023, People's Republic of China
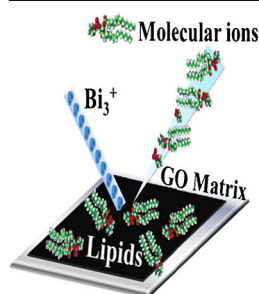
Abstract. Using matrix to enhance the molecular ion signals for biomolecule identification without loss of spatial resolution caused by matrix crystallization is a great challenge for the application of TOF-SIMS in real-world biological research. In this report, graphene oxide (GO) was used as a matrix for TOF-SIMS to improve the secondary ion yields of intact molecular ions ($[M + H]^+$). Identifying and distinguishing the molecular ions of lipids ($m/z > 700$) therefore became straightforward. The spatial resolution of TOF-SIMS imaging could also be improved as GO can form a homogeneous layer of matrix instead of crystalline domain, which prevents high spatial resolution in TOF-SIMS imaging. Lipid mapping in presence of GO revealed the delicate morphology and distribution of single vesicles with a diameter of 800 nm. On GO matrix, the vesicles with similar shape but different chemical composition could be distinguished using molecular ions. This novel matrix holds potentials in such applications as the analysis and imaging of complex biological samples by TOF-SIMS.

Keywords: TOF-SIMS, Matrix enhancement, Graphene oxide, Molecular ions, Bio-imaging

Introduction

Imaging mass spectrometry (IMS) as a unique technique offers both spatial and chemical composition information of biomolecules present in tissues or cells [1–4]. Matrix-assisted laser desorption/ionization mass spectrometry (MALDI-MS) has been widely used in tissue imaging and proteomic analysis, allowing the detection of large molecules up to 100 kDa [5–7]. The spatial resolution of MALDI-MS, which can reach ~30–100 μm, is determined by the laser spot size as well as the matrix crystals [8–10].

Time-of-flight secondary ion mass spectrometry (TOF-SIMS) has emerged as a powerful tool to map low-mass (<500 Da) biomolecules in single cell or subcellular level [2,

11, 12] at a routinely submicrometer spatial resolution. Impressively, Ewing et al. [11] mapped the headgroup fragmental ions of lamellar lipidsphosphocholine and nonlamellar 2-aminoethylyphosphonolipid from Tetrahy-mena using TOF-SIMS and revealed the formation of domains in response to structure changes of lipids during cell-to-cell conjugation. Sweedler et al. [12] showed by TOF-SIMS imaging that vitamin E localized at the junction of the soma and neurite in a single neuron cell. The results provided evidence for the theory that reduced axonal transport in cells was caused by the lack of vitamin E. Compared with conventional IMS, TOF-SIMS offered high sensitivity, chemical specificity, and submicrometer spatial resolution, and emerged as a promising method to answer life science questions [13, 14].

However, TOF-SIMS often suffers from severe molecular fragmentation in the analysis of large biomolecules as it uses a high-energy primary ion beam normally at primary ion doses ranging from 10^{10} to 10^{12} ions/cm² [15, 16]. As the energy is directly transferred from primary ions to analytes, the fragmentation dominates over the desorption/ionization process, resulting in the rapid reduction of molecular ions with

Correspondence to: Zhanping Li; *e-mail:* zhanpingli@tsinghua.edu.cn, Xinrong Zhang; *e-mail:* xrzhang@tsinghua.edu.cn

increasing mass [16]. Therefore, it is difficult to identify the origin of the small molecule fragments. For example, the peak of *m/z* 184 is characteristic of lipids in TOF-SIMS, which is attributed to the phosphocholine headgroup and other species of lipid molecules [2, 17, 18]. Therefore, detection of intact molecular ions rather than their fragments is the key to advance the applicability of TOF-SIMS in biological analysis.

Mapping molecular ions of high-mass biomolecules is quite difficult without matrix owing to insufficient sensitivity in TOF-SIMS [19]. Matrix-enhanced secondary ion mass spectrometry (ME-SIMS) relies on the matrix-enhanced desorption/ionization process, which combines the advantages of SIMS, FAB (Fast Atom Bombardment), and MALDI [15] to realize the detection of intact molecular ions of high-mass biomolecules (such as peptides, 1000–2500 Da [20, 21] and lipids, 700–900 Da [22, 23]). Primary ions are formed with lower energy in ME-SIMS, which leads to preferential ionization of the analyte ions and higher molecular ion yields [16, 24]. The most popular and efficient matrix for ME-SIMS is 2,5-dihydroxybenzoic acid (2,5-DHB) [15, 16, 20–22], a conventional MALDI matrix. Molecular ions of cholesterol and neuropeptide from cryosections of the cerebral ganglia of the freshwater snail [15] and intact glycerophospholipid ions from mammalian nervous tissue [25] were imaged by ME-SIMS both using 2,5-DHB as matrix. However, it is widely recognized that crystallization of matrix leads to the loss of ultimate spatial resolution, which is the limit of high spatial resolution in ME-SIMS [10, 26].

Metal assisted SIMS (Meta-SIMS) was also used to improve the secondary ion yield of intact molecules [19, 27, 28]. Altelaar and co-workers [27] successfully imaged the molecular ions of lipids between *m/z* 700 and 900 in tissue and a single neuroblastoma cell by coating a thin gold layer on the sample surface. In Meta-SIMS, analyte signals are commonly observed as compound-specific metal adducts such as Ag-cationized cholesterol at *m/z* 493–496 [28] or $[M_n+Au_m]^+$ of cholesterol and lipids [27]. The main impediment of sample metallization is the difficulty in peak assignment caused by metal adduct ion formation and image interpretation [19].

Graphene (G) and graphene oxide (GO) are two-dimensional (2D) carbon allotrope [29]. G was introduced as a matrix for matrix-assisted laser desorption/ionization time-of-flight mass spectrometry (MALDI-TOF MS) in 2010 [30] and further applied in imaging rat brain sections and soybean leaves [31]. It was proposed that graphene showed good performance, such as reducing fragmentation, high tolerance for salt, and low background signal in the mass spectra when serving to desorb and ionize polar and nonpolar compounds. Meanwhile, this material exhibited a better desorption/ionization performance for nonpolar compounds than traditional MALDI matrices [30]. Similarly, GO has also been used as a dual platform for both enrichment and ionization of fatty acids [32] and cocaine [33] in MALDI.

However, G and GO have never been used as a matrix in TOF-SIMS to enhance intact biomolecular ion signals. In this work, we found that GO as a TOF-SIMS matrix could significantly improve secondary ion yields of intact molecular ions of lipids. Different species of phospholipids with the same headgroup were identified by abundant $[M + H]^+$ signals in the mixture of standard lipids and lipid extract from human blood in the presence of GO matrix by TOF-SIMS. Moreover, GO formed a homogeneous layer without crystalline domain, reducing the impact on spacial resolution owing to matrix crystallization. We mapped $[M + H]^+$ signals of lipids from 800 nm vesicles made up of different species of lipids. The clear morphology and distribution of single vesicles were obtained with accurate chemical composition. Enhancement of intact molecular ions signals without loss of high spatial resolution suggests that GO is a promising matrix to be used in biological analysis by TOF-SIMS.

Experimental

Chemicals and Reagents

The samples of lipids, including 1-palmitoyl-2-oleoyl-*sn*-glycero-3-phosphocholine (POPC), 1,2-dioleoyl-*sn*-glycero-3-phosphocholine (DOPC), sphingomyelin d18:0/16:1 (SM), and PBS buffer were purchased from Sigma-Aldrich (St. Louis, MO, USA). The traditional matrix for MALDI α-cyano-4-hydroxycinnamic acid (CHCA), 2,5-dihydroxy-benzoic acid (DHB), and sinapic acid (SA) were purchased from Bruker Daltonics (Billerica, MA, USA). G and GO were purchased from Nanjing XFNANO Materials Tech Co., Ltd. (Nanjing, China). Chloroform, methanol, dichloromethane, and acetone were at HPLC grade and the water was prepared from a Milli-Q water (Millipore, Billerica, MA, USA) purification system.

Preparation of Analyte Solutions

Standard solutions of POPC, DOPC were prepared by dissolving in CHCl_3, and SM were prepared by dissolving in methanol at desired concentrations. The traditional MALDI matrices were prepared by dissolving in water (DHB 20 mg/mL, CHCA saturated solution, SA 20 mg/mL). G and GO were dissolved in water at a series of concentrations followed by ultrasonic dispersion. The matrix and analyte solutions were premixed to the same volume ratio (v/v = 1/1, typically 10 uL/10 uL).

Extraction of Total Lipids from Human Plasma

Blood samples were contributed by healthy adult volunteers who gave their informed consent. A simple MeOH method was used here to extract lipids from human plasma [34]. In brief, 10 μL plasma was added to 1 mL of MeOH followed by vortexing and incubation on ice for 10 min. Then the mixture was centrifuged (10,000 *g*, 5 min, room temperature) and the supernatant was obtained as the extraction of total lipids from human plasma.
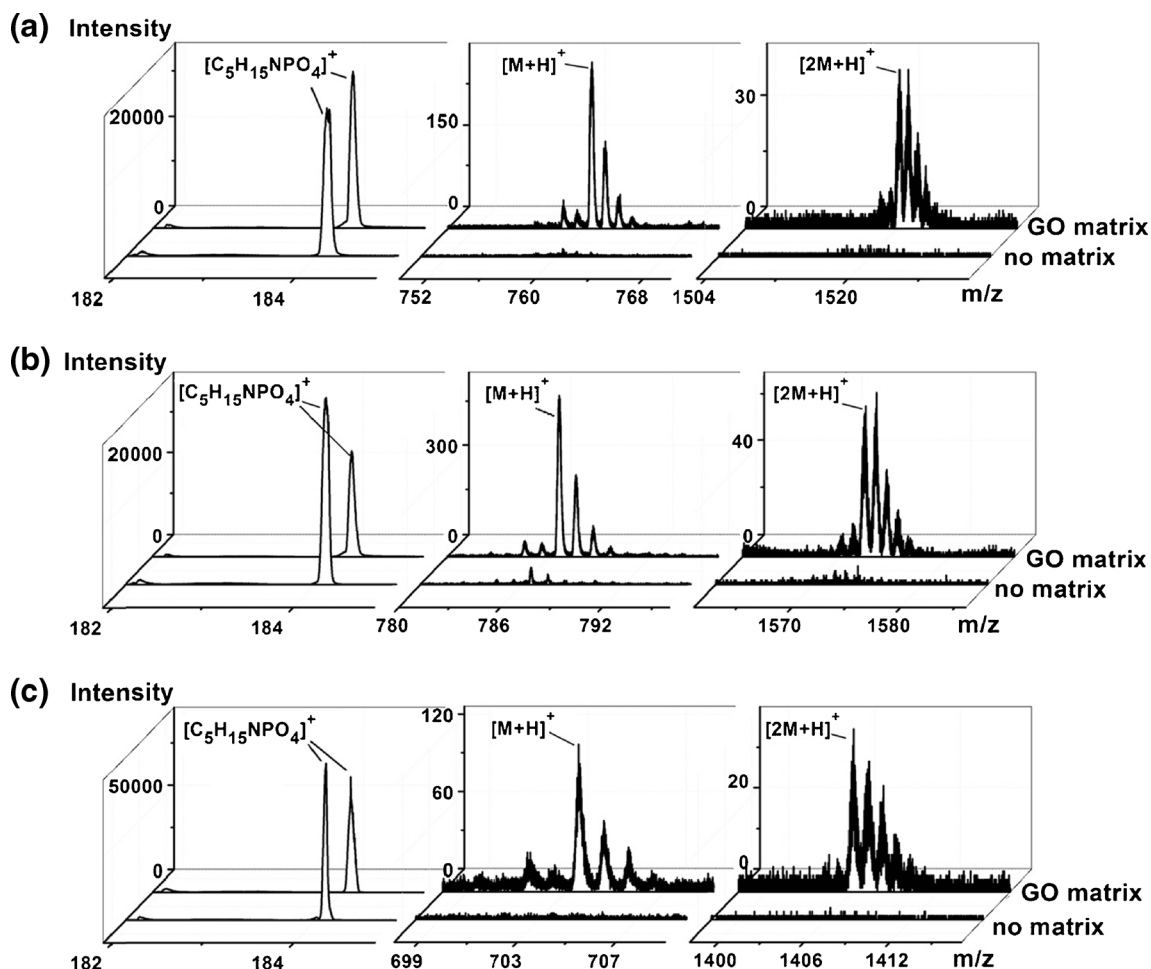
Figure 1. Fragmental and intact molecular ion signals in positive ion mode of (**a**) POPC, (**b**) DOPC, and (**c**) SM using GO as TOF-SIMS matrix or without matrix. Left to right respectively: fragmental ion ([$C_5H_{15}NPO_4$]$^+$ at m/z 184.1), molecular ion ([M + H]$^+$, POPC at m/z 760.5, DOPC at m/z 786.6, and SM at m/z 703.5) and bimolecular ion ([2 M + H]$^+$) signals

Preparation of 800 nm Lipid Vesicles

The common extrusion method was used to obtain lipid vesicles. In brief, POPC was first dissolved in chloroform to give a concentration of 1 mg/mL. Then the chloroform was evaporated under a stream of nitrogen gas, and followed by vacuum drying overnight to remove remaining chloroform. Next, the lipids were hydrated in deionized water and extruded through a 800 nm pore-size polycarbonate membrane filter (Avanti Polar Lipids, Alabaster, AL, USA) for 21 times. After diluting to 100-fold in deionized water, the vesicles dispersed suspension was mixed with GO solution to a same volume ratio or dropped on GO matrix covered wafer and dried at room temperature.

Sample Preparation for TOF-SIMS

The Si wafer were washed by water, dichloromethane, acetone, and methanol. The analyte solutions were directly dropped on a Si wafer with GO coating or premixed with matrix and dropped on Si wafer. They were dried at room temperature and then followed by TOF-SIMS analysis.

Mass Spectrometry

TOF-SIMS used in this study is TOF-SIMS 5 (ION-TOF GmbH, Münster, Germany) equipped with a Bi liquid metal ion gun (LMIG), or alternatively, collected TOF-SIMS spectra and images of standard samples using a 30 keV Bi$_3^+$ LMIG with a high mass resolution (HMR) mode and imaged submicrometer lipid vesicles with a high spatial resolution (HSR) mode. The Bi$_3^+$ current in the HMR mode was 0.8 pA (<1 ns pulse width, bunched beam), higher than 0.1 pA (100 ns pulse width, unbunched beam) in the HSR mode. The total Bi$_3^+$ accumulated ion dose was between 10^{11} and 10^{12} ions/cm^2 in the HMR mode whereas about 2.0×10^{10} ions/cm^2 was in HSR mode. The secondary ion images were acquired using Bi$_3^+$ LMIG rastering over a 100 × 100 μm^2 area with 128 × 128 pixels consistently, except the vesicles images with 256 × 256 pixels. The Bi$_3^+$ LMIG was operated at a cycle time 150 μs (mass range: 0 ~2000 u). Positive spectra were mass-calibrated using CH$_3^+$, C$_2$H$_3^+$, C$_2$H$_5^+$, C$_3$H$_5^+$, C$_4$H$_7^+$, and C$_5$H$_9^+$. The mass resolutions (measured at C$_2$H$_3^+$, m/z 27) were typically >6000 and the typical probe sizes of the Bi$_3^+$ LMIG was ~5 um in the HMR mode while ~200 nm in HSR mode for a higher spatial
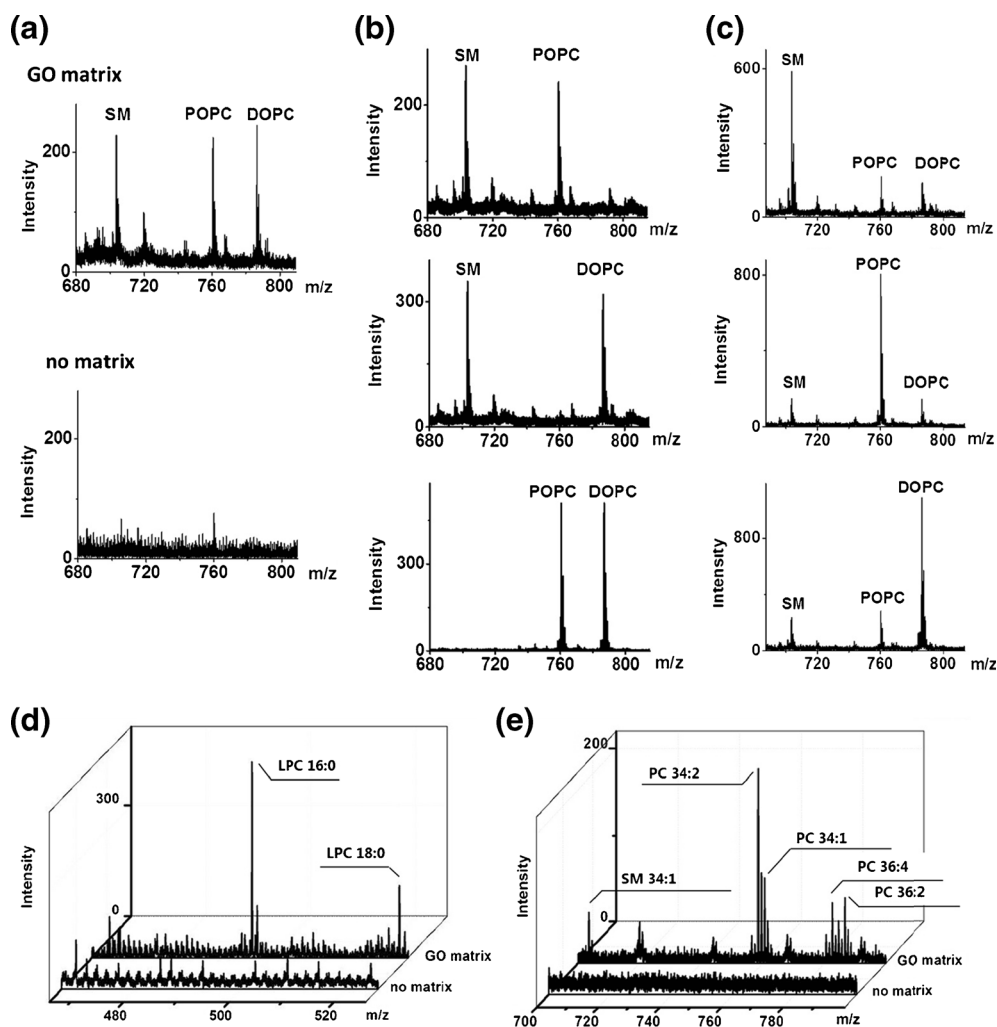
Figure 2. Intact molecular ion signals in positive ion mode from mixed lipid samples: (**a**) SM, POPC and DOPC at molar ratio 1/1/1 using GO matrix or without matrix, (**b**) two species of lipids mixture from the top down, SM and POPC, SM and DOPC, POPC and DOPC at molar ratio 1/1 with GO matrix, (**c**) three species of lipids mixture from the top down, SM, POPC, and DOPC at molar ratio 4/1/1; 1/4/1 and 1/1/4 with GO matrix. The lipid extraction from human plasma samples using GO as TOF-SIMS matrix or not: (**d**) some lysophosphatidylcholines in low-mass range, and (**e**) a series of phospholipids in higher-mass range

resolution. A flood gun with low energy electrons was used to compensate for charge buildup on sample surface.

Results and Discussion

Lipids Analysis Using GO as Matrix

When GO (8 mg/mL matrix solution) was used as the matrix in TOF-SIMS, the intense $[M + H]^+$ ion signals from POPC, DOPC, and SM, three typical kinds of phosphocholine in cells, were obtained. As shown in Figure 1, the $[M + H]^+$ ion signals at m/z 760.5, 786.6, and 703.5 from POPC, DOPC, and SM were all enhanced. The intensity of molecular ion signals increased >40-fold for POPC, >10-fold for DOPC, and ~40-folds for SM in repeated analysis (see SupplementaryTable S1). To further estimate the performance of GO to soften the ionization

conditions for biomolecules, taking POPC as an example, the intensity of the $[M + H]^+$ ion relative to that of the $[C_5H_{15}NPO_4]^+$ was much higher than that without matrix, 0.02 as opposed to 0.0006 for TOF-SIMS without GO. This result was similar to previous study, in which 2,5-DHB was used as matrix in TOF-SIMS [16]. Clearly, using GO matrix could evidently soften the ionization conditions for biomolecules. In contrast, whether using GO matrix or not, the phosphocholine headgroup at m/z 184.1 ($[C_5H_{15}NPO_4]^+$) was one of the most intense peaks existing in all positive ion mode spectra from POPC, DOPC, and SM. In negtive mode, $[M - H]^-$ signals of some lipids such as POPC were difficult to observe as showed in previous research [16].

In addition, the relative amount of GO and analytes made difference to the final secondary ion yield of molecular ions. When 10 μM POPC stock solution was premixed
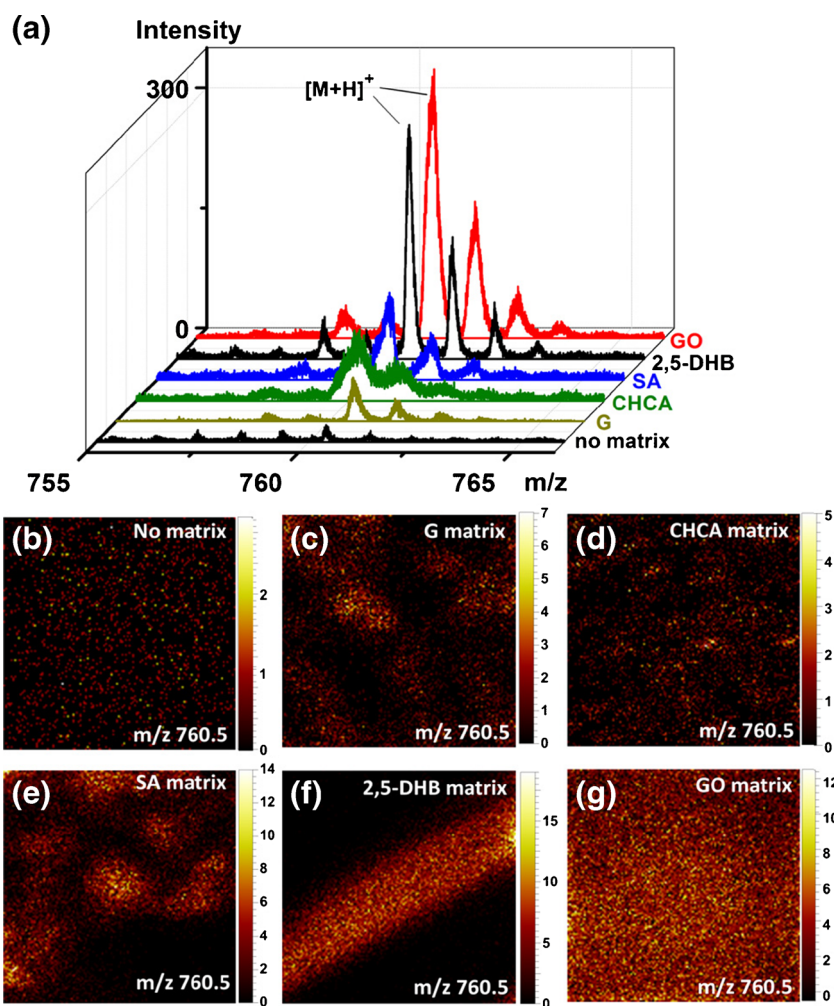
Figure 3. (a) Positive mode SIMS spectra of POPC [M + H]⁺ ions using different matrices: G, CHCA, SA, 2,5-DHB, GO or without matrix. TOF-SIMS images of POPC [M + H]⁺ ions in 100 μm × 100 μm scans using different matrices: (b) no matrix, (c) G, (d) CHCA, (e) SA, (f) 2,5-DHB, (g) GO

with GO matrix solution (v/v = 1/1), [M + H]⁺ ion signals of POPC gradually increased with the increase of GO concentration up to 6 mg/mL and then reached a plateau (see Supplementary Figure S1 and Supplementary Table S2). The control group showed uniformly weak [M + H]⁺ ion signals as background from the GO matrix solutions at the same concentration gradient without analyte. Moreover, the analytes distributed uniformly with matrix at a low GO concentration (up to 8 mg/mL) but became non-uniform and aggregated to blocks when GO concentration increased over 9 mg/mL (see Supplementary Figure S1). Therefore, a befitting final molecular ratio of GO and analytes should be chosen to ensure the effective enhancement of [M + H]⁺ ion signals and uniform distribution of analytes in matrix. In all of the following experiments, 8 mg/mL was used as the working concentration of GO matrix solution.

To imitate the complex composition in real biological system, a mixture solution of lipids was analysed. In Figure 2a, the intensity of molecular ion signals were

insufficient to distinguish when equimolar quantities of POPC, DOPC, and SM were mixed. When GO matrix was added to the sample, intense [M + H]⁺ ion signals from each lipid were obtained with approximately equal intensity. Similar results were observed with only two lipids as seen in Figure 2b. Moreover, the analysis of mixed sample with the molar ratio 4/1/1 showed a different intensity of [M + H]⁺ ion signals as shown in Figure 2c. These results demonstrated that using GO as a matrix in TOF-SIMS significantly enhanced the molecular ion signals of lipids to distinguish different lipids with the same headgroup. It was also applicable to analyze the diverse content of each lipid in mixed samples.

In a further investigation, lipids extracting solution from human serum samples were analyzed with GO matrix. Intense [M + H]⁺ ion signals from SM 34:1, PC 34:1, PC 36:2, and other phospholipids such as PC 34:2 at *m/z* 758.6, PC 36:4 at *m/z* 782.6, and PC 36:3 at *m/z* 784.6 were observed (Figure 2e). In addition, [M + H]⁺ ion signals from important signaling molecules in serum with
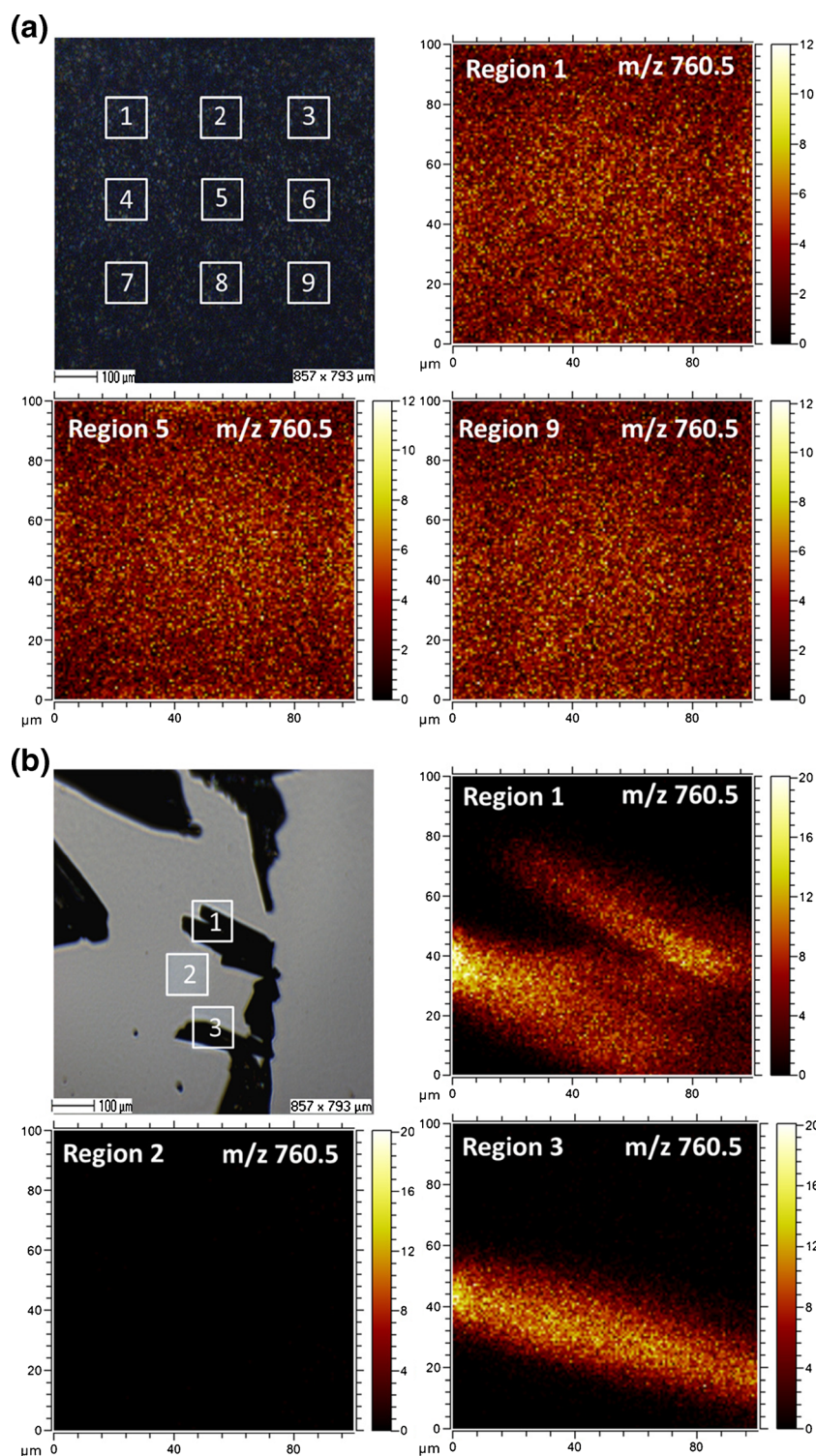
Figure 4. (a) Optical photograph (857 μm × 793 μm) of POPC with GO matrix using a built-in camera of TOF-SIMS and 100 μm × 100 μm 2D TOF-SIMS images of *m/z* 760.5 from region 1, region 5, region 9 with GO matrix; (b) 857 μm × 793 μm optical photograph of POPC with 2,5-DHB matrix and 100 μm × 100 μm 2D TOF-SIMS images of *m/z* 760.5 from region 1, region 2, region 3 with 2,5-DHB matrix

lower molecular weight such as lysophosphatidylcholine (LPC 16:0 at *m/z* 496.2 and LPC 18:0 at *m/z* 524.4) were obtained when GO matrix was used (Figure 2d). Intense signals at *m/z* 496.2 indicated the abundant amount of LPC 16:0 in serum, which was consistent with previous studies [34, 35]. Moreover, full information of lipidomics in plasma were obtained with a lot of identifiable molecular ion peaks. These peaks mainly derived from cholesterol,
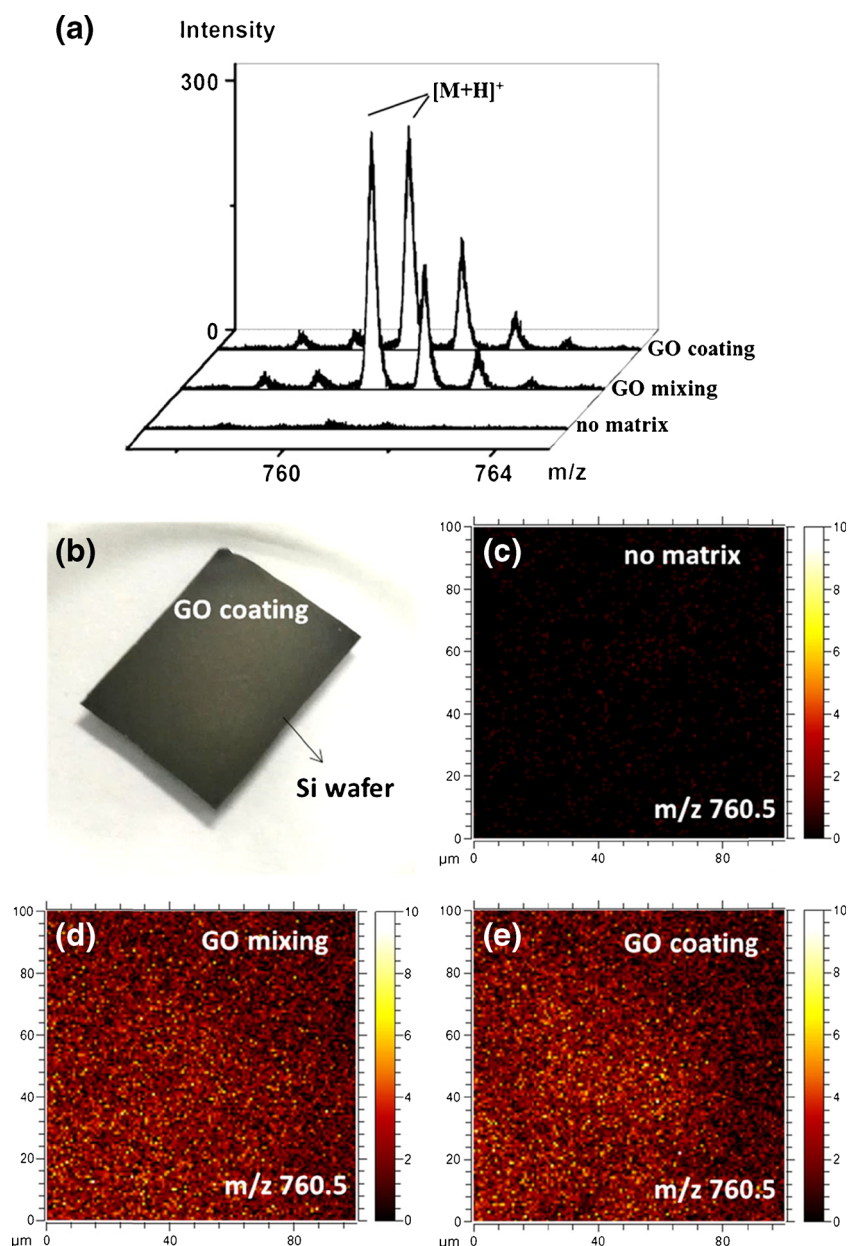
Figure 5. Detection and imaging [M +H]$^+$ ion signals using different sampling methods. (**a**) Positive mode SIMS spectra of POPC [M + H]$^+$ ions using GO matrix in different methods or without matrix. (**b**) The Si wafer with an evenly GO coating. The 100 μm × 100 μm 2D TOF-SIMS images of m/z 760.5 from POPC, (**c**) without matrix, (**d**) using GO in solution mixing method, and (**e**) dropped on Si wafer with GO coating

lysophospholipids, monoacylglyceride, diacylglyceride, and phospholipids (Supplementary Table S4). The results illustrated that GO was utilized not only as a matrix to soften the ionization process to detect intact molecular ion signals of high molecular mass lipids in TOF-SIMS but also enhanced the signals of lower molecular mass lipids. It is possible that the GO matrix enhanced the lipid extraction efficiency, which contributed to the higher detection of lipid species. Moreover, GO could also enhance the molecular ion signals of other high-mass biomolecules such as peptides (>1000 Da, see Supplementary Figure S2).

Uniform Distribution of GO Matrix for Imaging

To compare the analyte distribution in different matrices, GO, G, and 2,5-DHB, SA and CHCA were compared with POPC as analyte. The results showed that all the [M + H]$^+$ signals of POPC enhanced using those matrices than that without matrix (Figure 3a). As seen in Figure 3a, similar intense [M + H]$^+$ ion signals of POPC at m/z 760.5 were obtained due to the significant enhancement effect of both GO and 2,5-DHB matrix. When using G, CHCA, or SA as matrix, [M + H]$^+$ ion signals were much lower than that when using GO and 2,5-DHB. From Figure 3f and g, we also found that [M + H]$^+$ ion of
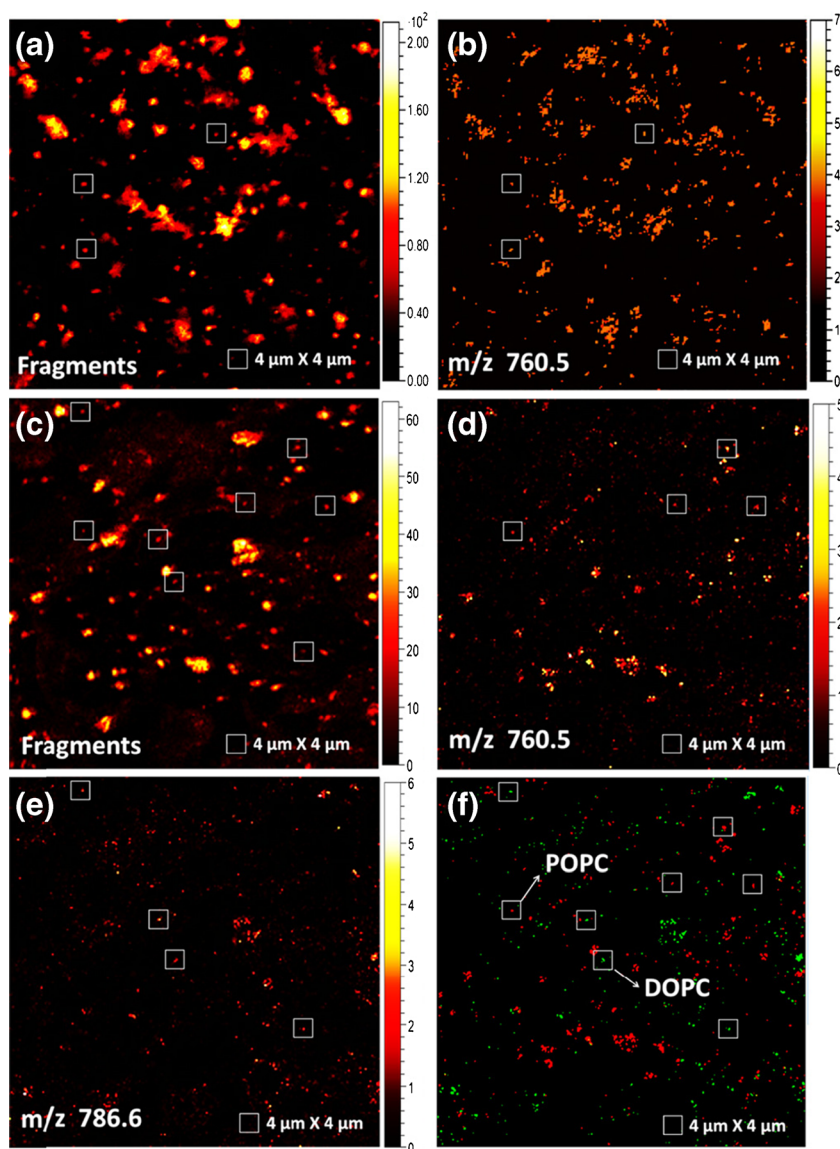
Figure 6. 100 μm × 100 μm 2D TOF-SIMS images of (**a**) the fragment, sum of m/z 86 and 184.1, and (**b**) [M + H]$^+$ of POPC at m/z 760.5 from single 800 nm POPC vesicles mixed with GO matrix; 100 μm × 100 μm 2D TOF-SIMS images of (**c**) the fragment, sum of m/z 86 and 184.1, (**d**) [M + H]$^+$ of POPC at m/z 760.5, (**e**) [M + H]$^+$ of DOPC at m/z 786.6, and (**f**) RGB overlay of m/z 760.5 (red) and m/z 786.6 (green) from 800 nm POPC vesicles and DOPC vesicles mixture dropped on Si wafer with GO coating

analyte distributed homogeneously with GO matrix but not with crystalline 2,5-DHB. G, CHCA, and SA also showed the non-uniform signal distribution of [M + H]$^+$ ions (see Figure 3c, d, and e). G is poorly soluble in water at room temperature and easy to form fragmental bulks after drying, leading to non-uniform distribution and different intensities of analytes in a scan area. The other matrices, CHCA and SA, showed a similar effect as G due to the different degrees in matrix crystal characteristics. The signal intensity of [M + H]$^+$ ion with GO as matrix was similar to that using 2,5-DHB while GO formed a homogeneous and continuous phase matrix, dispersing the analyte uniformly in matrix.

Homogeneous distribution and high spatial resolution images of intact molecular ion signals from lipids were obtained mainly due to the formation of an evenly continuous phase and enhancement effect of GO.

To further investigate the analyte distribution in a larger area with GO matrix, molecular ion signals of POPC were imaged from nine square regions (100 μm × 100 μm) in a 857 μm × 793 μm scan area. GO homogeneously covered all optical scan area (857 μm × 793 μm) without crystallization phenomenon (Figure 4a). The intense [M + H]$^+$ ion signals of POPC at m/z 760.5 were obtained uniformly from each region

with GO matrix. The TOF-SIMS 2D images of *m/z* 760.5 from region 1, region 5, and region 9 are shown in Figure 4a as representative, and the other regions show similar images in Supplementary Figure S3. Homogeneous distribution of intense $[M + H]^+$ ion signals in all scan areas were observed from all images. However, when using 2,5-DHB as matrix, the $[M + H]^+$ ion signals were only observed in crystalline domain, resulting in a heterogeneous distribution of $[M + H]^+$ ion signals in images, as shown in Figure 4b.

To facilitate the application of GO as a matrix for TOF-SIMS imaging, another sample preparation method was also adopted. By virtue of its material characteristics, covering GO on a Si substrate surface could form an evenly continuous coating as a bottom matrix for TOF-SIMS. First, GO solution was dropped on Si wafer and formed a film after drying, evenly covering the surface of Si wafer as shown in Figure 5b. Then the analyte solution was dropped on this matrix.

In this way, the intense signals and uniform distribution of POPC $[M + H]^+$ ions on GO matrix were similar to that in solution premixing method (see Figure 5). The results indicated that GO as a matrix could ensure uniform distribution of analytes with matrix in different sample preparation methods and may avoid the limitation of spatial resolution due to matrix crystallization for imaging in ME-SIMS.

Imaging Lipid Vesicles Using GO Matrix

Lipid vesicles are small bubbles of amphiphilic lipid molecules [36], and widely used in biomedicine and biochemistry [37, 38]. Optical electronic microscope [39] and atomic force microscope [40] can image microtopography with precise size of these vesicles, but incapable of offering molecular information. Many prior reports of imaging lipid vesicles relied on detecting fragment ions such as $[C_5H_{12}N]^+$ and $[C_5H_{15}NPO_4]^+$ in TOF-SIMS analysis [41, 42]. In this work, with enhancement of intact molecular ion signals by using GO matrix (see Supplementary Figure S4c and d), POPC vesicles with a diameter of 800 nm could be imaged by using $[M + H]^+$ signals to show the delicate morphology and identify the chemical composition of vesicles. In the image of $[M + H]^+$ signals of POPC (Figure 6b), three single vesicles are shown in 4 μm × 4 μm white boxes, which are at the same locations in the image of fragmental ion signals (see Figure 6a). TOF-SIMS images of the fragmental ion signals, sum of *m/z* 86.1 and *m/z* 184.1 ($C_5H_{12}N^+$ and $C_5H_{15}NPO_4^+$) also show the solo vesicles with clear morphology (Supplementary Figure S4a), but the intensity of $[M + H]^+$ ion signals is insufficient to image the vesicles without matrix (Supplementary Figure S4b). The results illustrate that GO matrix enables the imaging of molecular ion signals of POPC vesicles and uniform distribution of analytes without the sacrifice of high spatial resolution of TOF-SIMS.

Moreover, the mixture of POPC vesicles and DOPC vesicles was dropped on the Si wafer with GO coating and freeze-dried. Imaging the fragmental ions showed all vesicles distribution (Figure 6c) but was unable to distinguish the species of vesicles. When mapping the molecular ions of POPC (Figure 6d) and DOPC (Figure 6e), respectively, the TOF-SIMS images showed the different distribution of these two vesicles. As shown in Figure 6f, the delicate morphology and distribution of single POPC vesicle (red) and single DOPC vesicle (green) could be observed at submicrometer size simultaneously and it was easy to distinguish the species of these vesicles according to the molecular ion signals. Without matrix, the weak $[M + H]^+$ signals (Supplementary Figure S5d) were insufficient to image POPC vesicles or DOPC vesicles (Supplementary Figure S5b and c) and the lipid vesicles could only be mapped by fragmental ion signals (Supplementary Figure S5a).

The results indicated that using GO as matrix for TOF-SIMS was a promising tool in lipidomics analysis to image lipid samples with submicrometer spatial resolution and identify lipid composition with accurate molecular weight of intact molecular ions.

Conclusion

In this work, GO was used as a TOF-SIMS matrix. Intact molecular ion signals of lipids were enhanced with GO attributable to the increased secondary ion yields of intact molecular ions. The enhanced detection of intact lipids and peptides suggests that GO is a promising matrix for TOF-SIMS analysis of biomolecules. In comparison to the traditional crystal matrix, GO can form a homogeneous layer and allow the continuous distribution of analytes, reducing the impact on spatial resolution of TOF-SIMS. Imaging intact lipid ions showed the clear morphology and chemical composition of lipid vesicles with a diameter of 800 nm. It is believed that using GO as the matrix for TOF-SIMS would allow the analysis of complex biosamples such as tissues, model membrane systems, or even single cells to further promote high-resolution MS imaging.

Acknowledgments

References

1. Chaurand, P., Schwartz, S.A., Billheimer, D., Xu, B.J., Crecelius, A., Caprioli, R.M.: Integrating histology and imaging mass spectrometry. Anal. Chem. **76**, 1145–1155 (2004)

2. Ostrowski, S.G., Van Bell, C.T., Winograd, N., Ewing, A.G.: Mass spectrometric imaging of highly curved membranes during Tetrahymena mating. Science **305**, 71–73 (2004)

3. Rohner, T.C., Staab, D., Stoeckli, M.: MALDI mass spectrometric imaging of biological tissue sections. Mech. Aging Dev. **126**, 177–185 (2005)

4. Lechene, C., Hillion, F., McMahon, G., Benson, D., Kleinfeld, A.M., Kampf, J.P., Distel, D., Luyten, Y., Bonventre, J., Hentschel, D., Park, K.M., Ito, S., Schwartz, M., Benichou, G., Slodzian, G.: High-resolution quantitative imaging of mammalian and bacterial cells using stable isotope mass spectrometry. J. Biol. **5**, 1–30 (2006)

5. Caprioli, R.M., Farmer, T.B., Gile, J.: Molecular imaging of biological samples: localization of peptides and proteins using MALDI-TOF MS. Anal. Chem. **69**, 4751–4760 (1997)

6. Cohen, S.L., Chait, B.T.: Influence of matrix solution conditions on the MALDI-MS analysis of peptides and proteins. Anal. Chem. **68**, 31–37 (1996)

7. Cornett, D.S., Reyzer, M.L., Chaurand, P., Caprioli, R.M.: MALDI imaging mass spectrometry: molecular snapshots of biochemical systems. Nat. Methods **4**, 828–833 (2007)

8. Kruse, R., Sweedler, J.V.: Spatial profiling invertebrate ganglia using MALDI MS. J. Am. Soc. Mass Spectrom. **14**, 752–759 (2003)

9. Khatib-Shahidi, S., Andersson, M., Herman, J.L., Gillespie, T.A., Caprioli, R.M.: Direct molecular analysis of whole-body animal tissue sections by imaging MALDI mass spectrometry. Anal. Chem. **78**, 6448–6456 (2006)

10. Luxembourg, S.L., Mize, T.H., McDonnell, L.A., Heeren, R.M.A.: High-spatial resolution mass spectrometric imaging of peptide and protein distributions on a surface. Anal. Chem. **76**, 5339–5344 (2004)

11. Kurczy, M.E., Piehowski, P.D., Van Bell, C.T., Heien, M.L., Winograd, N., Ewing, A.G.: Mass spectrometry imaging of mating Tetrahymena show that changes in cell morphology regulate lipid domain formation. Proc. Natl. Acad. Sci. U. S. A. **107**, 2751–2756 (2010)

12. Monroe, E.B., Jurchen, J.C., Lee, J., Rubakhin, S.S., Sweedler, J.V.: Vitamin E imaging and localization in the neuronal membrane. J. Am. Chem. Soc. **127**, 12152–12153 (2005)

13. Colliver, T.L., Brummel, C.L., Pacholski, M.L., Swanek, F.D., Ewing, A.G., Winograd, N.: Atomic and molecular imaging at the single-cell level with TOF-SIMS. Anal. Chem. **69**, 2225–2231 (1997)

14. Fletcher, J.S., Lockyer, N.P., Vaidyanathan, S., Vickerman, J.C.: TOF-SIMS 3D biomolecular imaging of *Xenopus laevis* oocytes using buck-minsterfullerene (c60) primary ions. Anal. Chem. **79**, 2199–2206 (2007)

15. Wu, K.J., Odom, R.W.: Matrix-enhanced secondary ion mass spectrometry: a method for molecular analysis of solid surfaces. Anal. Chem. **68**, 873–882 (1996)

16. Luxembourg, S.L., McDonnell, L.A., Duursma, M.C., Guo, X., Heeren, R.M.A.: Effect of local matrix crystal variations in matrix-assisted ionization techniques for mass spectrometry. Anal. Chem. **75**, 2333–2341 (2003)

17. Prinz, C., Höök, F., Malm, J., Sjövall, P.: Structural effects in the analysis of supported lipid bilayers by time-of-flight secondary ion mass spectrometry. Langmuir **23**, 8035–8041 (2007)

18. Roddy, T.P., Cannon, D.M., Ostrowski, S.G., Ewing, A.G., Winograd, N.: Proton transfer in time-of-flight secondary ion mass spectrometry studies of frozen-hydrated dipalmitoylphosphatidylcholine. Anal. Chem. **75**, 4087–4094 (2003)

19. McDonnell, L.A., Heeren, R.M.A.: Imaging mass spectrometry. Mass Spectrom. Rev. **26**, 606–643 (2007)

20. Altelaar, A.F.M., van Minnen, J., Jiménez, C.R., Heeren, R.M.A., Piersma, S.R.: Direct molecular imaging of *Lymnaea stagnalis* nervous tissue at subcellular spatial resolution by mass spectrometry. Anal. Chem. **77**, 735–741 (2005)

21. Korsgen, M., Pelster, A., Dreisewerd, K., Arlinghaus, H.F.: 3D ToF-SIMS analysis of peptide incorporation into MALDI matrix crystals with sub-micrometer resolution. J. Am. Soc. Mass Spectrom. **27**, 277–284 (2016)

22. McDonnell, L.A., Piersma, S.R., MaartenAltelaar, A.F., Mize, T.H., Luxembourg, S.L., Verhaert, P.D.E.M., van Minnen, J., Heeren, R.M.A.: Subcellular imaging mass spectrometry of brain tissue. J. Mass Spectrom. **40**, 160–168 (2005)

23. Fitzgerald, J.J.D., Kunnath, P., Walker, A.V.: Matrix-enhanced secondary ion mass spectrometry (ME SIMS) using room temperature ionic liquid matrices. Anal. Chem. **82**, 4413–4419 (2010)

24. Wittmaack, K., Szymczak, W., Hoheisel, G., Tuszynski, W.: Time-of-flight secondary ion mass spectrometry of matrix-diluted oligo- and polypeptides bombarded with slow and fast projectiles: positive and negative matrix and analyte ion yields, background signals, and sample aging. J. Am. Soc. Mass Spectrom. **11**, 553–563 (2000)

25. Lanni, E.J., Dunham, S.J.B., Nemes, P., Rubakhin, S.S., Sweedler, J.V.: Biomolecular imaging with a C-60-SIMS/MALDI dual ion source hybrid mass spectrometer: instrumentation, matrix enhancement, and single cell analysis. J. Am. Soc. Mass Spectrom. **25**, 1897–1907 (2014)

26. Rubakhin, S.S., Sweedler, J.V.: A mass spectrometry primer for mass spectrometry imaging. Methods Mol. Biol. **656**, 21–49 (2010)

27. Altelaar, A.F.M., Klinkert, I., Jalink, K., de Lange, R.P.J., Adan, R.A.H., Heeren, R.M.A., Piersma, S.R.: Gold-enhanced biomolecular surface imaging of cells and tissue by SIMS and MALDI mass spectrometry. Anal. Chem. **78**, 734–742 (2006)

28. Sjövall, P., Lausmaa, J., Nygren, H., Carlsson, L., Malmberg, P.: Imaging of membrane lipids in single cells by imprint-imaging time-of-flight secondary ion mass spectrometry. Anal. Chem. **75**, 3429–3434 (2003)

29. Zhu, Y., Murali, S., Cai, W., Li, X., Suk, J.W., Potts, J.R., Ruoff, R.S.: Graphene and graphene oxide: synthesis, properties, and applications. Adv. Mater. **22**, 3906–3924 (2010)

30. Dong, X., Cheng, J., Li, J., Wang, Y.: Graphene as a novel matrix for the analysis of small molecules by MALDI-TOF MS. Anal. Chem. **82**, 6208–6214 (2010)

31. Friesen, W.L., Schultz, B.J., Destino, J.F., Alivio, T.E.G., Steet, J.R., Banerjee, S., Wood, T.D.: Two-dimensional graphene as a matrix for MALDI imaging mass spectrometry. J. Am. Soc. Mass Spectrom. **26**, 1963–1966 (2015)

32. Liu, Y., Liu, J., Deng, C., Zhang, X.: Graphene and graphene oxide: two ideal choices for the enrichment and ionization of long-chain fatty acids free from matrix-assisted laser desorption/ionization matrix interference. Rapid Commun. Mass Spectrom. **25**, 3223–3234 (2011)

33. Gulbakan, B., Yasun, E., Shukoor, M.I., Zhu, Z., You, M., Tan, X., Sanchez, H., Powell, D.H., Dai, H., Tan, W.: A dual platform for selective analyte enrichment and ionization in mass spectrometry using aptamer-conjugated graphene oxide. J. Am. Chem. Soc. **132**, 17408–17410 (2010)

34. Zhao, Z., Xu, Y.: An extremely simple method for extraction of lysophospholipids and phospholipids from blood samples. J. Lipid Res. **51**, 652–659 (2010)

35. Takahashi, H., Goto, T., Yamazaki, Y., Kamakari, K., Hirata, M., Suzuki, H., Shibata, D., Nakata, R., Inoue, H., Takahashi, N., Kawada, T.: Metabolomics reveal 1-palmitoyl lysophosphatidylcholine production by peroxisome proliferator-activated receptor α. J. Lipid Res. **56**, 254–265 (2015)

36. Israelachvili, J.N., Mitchell, D.J., Ninham, B.W.: Theory of self-assembly of lipid bilayers and vesicles. Biochim. Biophys. Acta **470**, 185–201 (1977)

37. Guo, X., Szoka, F.C.: Chemical approaches to triggerable lipid vesicles for drug and gene delivery. Acc. Chem. Res. **36**, 335–341 (2003)

38. Walde, P., Ichikawa, S.: Enzymes inside lipid vesicles: preparation, reactivity and applications. Biomol. Eng. **18**, 143–177 (2001)

39. Cevc, G.: Lipid vesicles and other colloids as drug carriers on the skin. Adv. Drug Deliv. Rev. **56**, 675–711 (2004)

40. Richter, R., Mukhopadhyay, A., Brisson, A.: Pathways of lipid vesicle deposition on solid surfaces: a combined QCM-D and AFM study. Biophys. J. **85**, 3035–3047 (2003)

41. Gunnarsson, A., Kollmer, F., Sohn, S., Höök, F., Sjövall, P.: Spatial-resolution limits in mass spectrometry imaging of supported lipid bilayers and individual lipid vesicles. Anal. Chem. **82**, 2426–2433 (2010)

42. Sjövall, P., Agnarsson, B., Carlred, L., Gunnarsson, A., Höök, F.: Liposome binding for multiplexed biomolecule detection and imaging using ToF-SIMS. Surf. Interface Anal. **46**, 707–711 (2014)